Available online at www.sciencedirect.com
ScienceDirect
Energy Procedia 161 (2019) 259–267
Energy Procedia
www.elsevier.com/locate/procedia

2nd International Conference on Sustainable Energy and Resource Use in Food Chains, ICSEF 2018, 17-19 October 2019, Paphos, Cyprus

Analysis of an R744 typical booster configuration, an R744 parallel-compressor booster configuration and an R717/R744 cascade refrigeration system for retail food applications. Part 1: Thermodynamic analysis

Carlos Amaris[a], Konstantinos M. Tsamos[b]*, Savvas A Tassou[b]

[a]*University of Costa Rica, School of Chemical Engineering, , 11501-2060, San José, Costa Rica*
[b]*Brunel University London, Institute of Energy Futures, RCUK Centre for Sustainable Energy use in Food chains (CSEF), Uxbridge, UB8 3PH, United Kingdom*

Abstract

In this paper, the performances of a typical R744 booster configuration, a R744 parallel-compressor booster refrigeration system, and a R717/R744 cascade system configuration are presented based on the 1st and 2nd law of thermodynamics, for food retail applications. The results for a supermarket application with a total 145 kW cooling capacity show that the typical booster system and parallel-compressor booster system have better performances than the cascade system. However, for convenience store applications with 30 kW total cooling capacity the cascade system shows better performance beyond 26 °C ambient temperature which limits the applications of the cascade system for low capacity systems and the parallel refrigeration system solution appears to be a better option. In addition, the most critical components of each system based on the 2nd law are identified in this paper.

Keywords: Natural refrigerants; booster refrigeration system; cascade refrigeration system; energy analysis; exergy analysis.

* Corresponding author. Tel.: +44 1895 266659
E-mail address: konstantinos.tsamos@brunel.ac.uk

10.1016/j.egypro.2019.02.090

Nomenclature

casc_HE	Cascade heat exchanger	LT/ MT	Low/ Medium temperature
comp	Compressor	LTHE	Low temperature heat exchanger
COP	Coefficient of performance	$\dot{m}$	Refrigerant mass flow (kg/s)
e	Evaporator	P	Pressure (bar)
Eff	2nd Law Efficiency	PR	Pressure ratio
ev	Expansion valve	$\dot{Q}$	Cooling capacity (kW)
gc/c	Gas cooler/condenser	s	Entropy (kJ/kg K)
h	Enthalpy (kJ/kg)	T	Temperature (°C)
I	Irreversibility (kJ/s)	$\dot{W}$	Power consumption (kW)
LP/ MP	Low/ Medium pressure		

1. Introduction

The chilled food chain is responsible for a large amount of energy in refrigeration for the maintenance of low temperatures during processing, transportation and retail of chilled food products [1, 2]. Therefore, the use of environment-friendly and efficient refrigeration systems in the food chain is an actual need. Extensive work has been carried out on various R744 supermarket refrigeration systems including a typical booster configuration, parallel-compressor configuration, R744 configuration with ejectors and multi-ejector configuration with overfeed evaporators, all of them with the target of reducing the energy consumption of the system and indirect emissions. On the other hand, retailers are looking for simple, not expensive, easy to maintain and operable configurations to supply both low and medium temperature cooling. Two natural refrigerants, ammonia (R717) and carbon dioxide (R744) have each proven to be very effective refrigerants, R717 favouring large industrial systems and R744 the commercial retail sector. In terms of R717, its toxicity is high to be used within the retail area. In the case of R744, it is less efficient in high ambient temperature applications. However, the marriage of the two natural refrigerants within a single refrigeration system such as the cascade configuration, can offer safe operation and advantages that each refrigerant cannot deliver alone.

A number of recent studies report on multi-stage refrigeration systems which can be applied to food refrigeration. For instance, Lee et al. [3] conducted an energy and exergy analysis of a conventional R717/R744 cascade refrigeration system and found that at a cascade condensing temperature of -15 °C, evaporating temperature of -50 °C and a ΔT = 5 °C, a maximum COP of 1.15 can be reached. Meanwhile, Bingming et al. [4] experimentally compared the performances of a R717/R744 cascade refrigeration system, a two-stage R717 system and a single-stage R717 system with and without an economizer. The main output from this study was that the cascade configuration showed best performance at evaporating temperatures below -40 °C. Dopazo et al. [5] theoretically identified that for the R717/R744 cascade refrigeration system COP improves as the R744 evaporating temperature is increased and the R717 condensing temperature reduces. Rezayan and Behbahaninia [6] investigated the thermo-economic optimisation of the R717/R744 cascade refrigeration cycle. The author's study included thermal and economic aspects of the system design and operation. Based on the proposed design and operation of the system and for a constant cooling capacity of 40 kW, the annual cost reduction of the system was equal to 9.34% compared with the base case design. Messineo [7] compared a basic R744/R717 cascade system configuration with an R404A two-stage system based on similar operating conditions reporting similar performances. The experimental analysis of an R717/R744 cascade system configuration for supermarket refrigeration applications was presented by Sawalha [8]. The R744 refrigerant was used to cool-down the LT and MT where a DX and flooded coil were employed respectively. Sawalha concluded that the performance for the R717/R744 cascade solution was 50 to 60 % higher than that of a direct R404A system installed in the same laboratory environment.

In most of the published works the analysis involved only cascade refrigeration systems where the low-temperature stage circuit feeds only low-temperature evaporators [9-13]. Other studies available in the open literature present analyses of different system arrangements with R744 as a single refrigerant [14]. The sensitivity analysis of a conventional R744 booster refrigeration system was presented by Ge and Tassou [15]. In this study, the ambient temperature, the effectiveness of the internal heat exchanger located downstream the condenser/gas cooler and the isentropic efficiency of the high-temperature stage compressors were reported to be the most critical parameters determining optimal gas cooler pressure. More recently, Gullo et al. [16-18] reported on the thermodynamic performance of various R744 booster refrigeration systems including parallel compression at different ambient temperatures. In those studies, the authors highlighted that special attention should be paid to the design of the gas cooler/condenser, the high stage compressor and the medium temperature evaporator [16]. They also mentioned the convenience of using parallel compression and dedicated sub-cooling at the outlet of the gas cooler/condenser [17] or multi-ejector units [18]. Lastly, Mylona et al. [19] discussed a comparative analysis of the energy use and environmental impact of different refrigeration systems for frozen food supermarket application. The existing remote plugged-in system was compared against various centralised systems including two parallel MT and LT systems, two MT and LT parallel cascade systems with R134a/CO2 and finally a trans-critical booster system. The authors concluded that besides these refrigeration systems, the CO2 booster trans-critical appears the most promising replacement due to its high efficiency at London climate conditions.

In this paper the energy performances, based on 1st and 2nd thermodynamic law analysis, of a typical R744 booster configuration, a R744 parallel-compressor booster refrigeration system, and a R717/R744 cascade system configuration involving two temperature levels for food retail applications are presented. It includes the estimation of the coefficient of performance, power consumption and irreversibility in each system at ambient temperatures ranging from 0 to 40 ºC. In addition, the most critical components of each system based on the 2nd law are identified.

2. Description of the systems

Fig. 1 shows a schematic diagram of an R744 typical booster refrigeration system, an R744 parallel-compressor refrigeration system, and an R717/R744 cascade refrigeration system, all of them with two temperature levels, for food retail applications. A scheme of a typical R744 booster refrigeration system is presented in Fig. 1a. The detailed description of the system is presented in [14].

The system can operate in both subcritical and trans-critical modes depending on the ambient temperature. The refrigerant from the LT evaporator outlet is drawn into the first stage low-stage compressor suction line. The discharge from the LP compressor mixes with the outlet of the MT evaporator, point 1. Before the mixed refrigerant enters the suction line of the high-temperature stage compressors and compressed to gas cooler/condenser pressure, it is mixed with the gas by-pass refrigerant from the R744 liquid receiver. At that stage, the pressure is controlled by the HP expansion valve and the variable speed fan of the gas cooler/condenser. The most common disadvantage of this system is the reduction of COP due to the higher quantities of flash gas by-pass and the higher pressures which lead to higher electrical power consumptions.

The diagram of a R744 parallel-compressor booster refrigeration system is presented in Fig. 1b. As in the previous system, the parallel-compressor booster system can also operate in both subcritical and trans-critical modes depending on the ambient temperature. In Fig. 1b can be observed that the main difference of this present system with respect to the typical system, in Fig 1a, is the use of a by-pass compressor instead of the by-pass valve. In this case the discharge of the compressor is located at the mix point 2 where the refrigerant mixes with the flow coming from the HP compressor. For this configuration, the pressure is also controlled by the HP expansion valve and the variable speed fan of the gas cooler/condenser.

The scheme of the R717/744 cascade refrigeration system is shown in Fig. 1c. It consists mainly of two loops: the upper-side loop fed with R717 and lower-side with R744 as working fluid. Both sides are exchanging heat through the cascade heat exchanger which operates as an evaporator for the R717 side and condenser for the R744 side. The cascade system solution guarantees a subcritical operation all year around for the R744 system and higher performance when this is used in warm climate applications. Additionally, the high-pressure R744 expansion valve is no longer required due to the low condensation temperature of the R744. The upper-side loop consists of an R717 screw compressor, an air-cooled condenser, an expansion valve, and the upper side of the cascade heat exchanger (evaporator).

The R744 low-side consists of a liquid receiver, and direct expansion (DX) medium temperature (MT) and low temperature (LT) evaporators. In order to control the pressure difference between the LT and MT side, a double stage compression is employed. As seen in Fig. 1c, a solenoid valve and by-pass valve are installed (in series) after the liquid receiver (between points 7 and 8). This is an additional safety factor and will be used in order to by-pass the R744 fluid from the liquid receiver to the suction of the compressor to prevent any over-pressure on the system when is needed. In addition, a heat exchanger (HX) is used for sub-cooling the R744 flow before entering the LT expansion valve and to ensure superheated vapour at the suction line of the low-pressure compressor. More details about the cascade system can be found in [20].

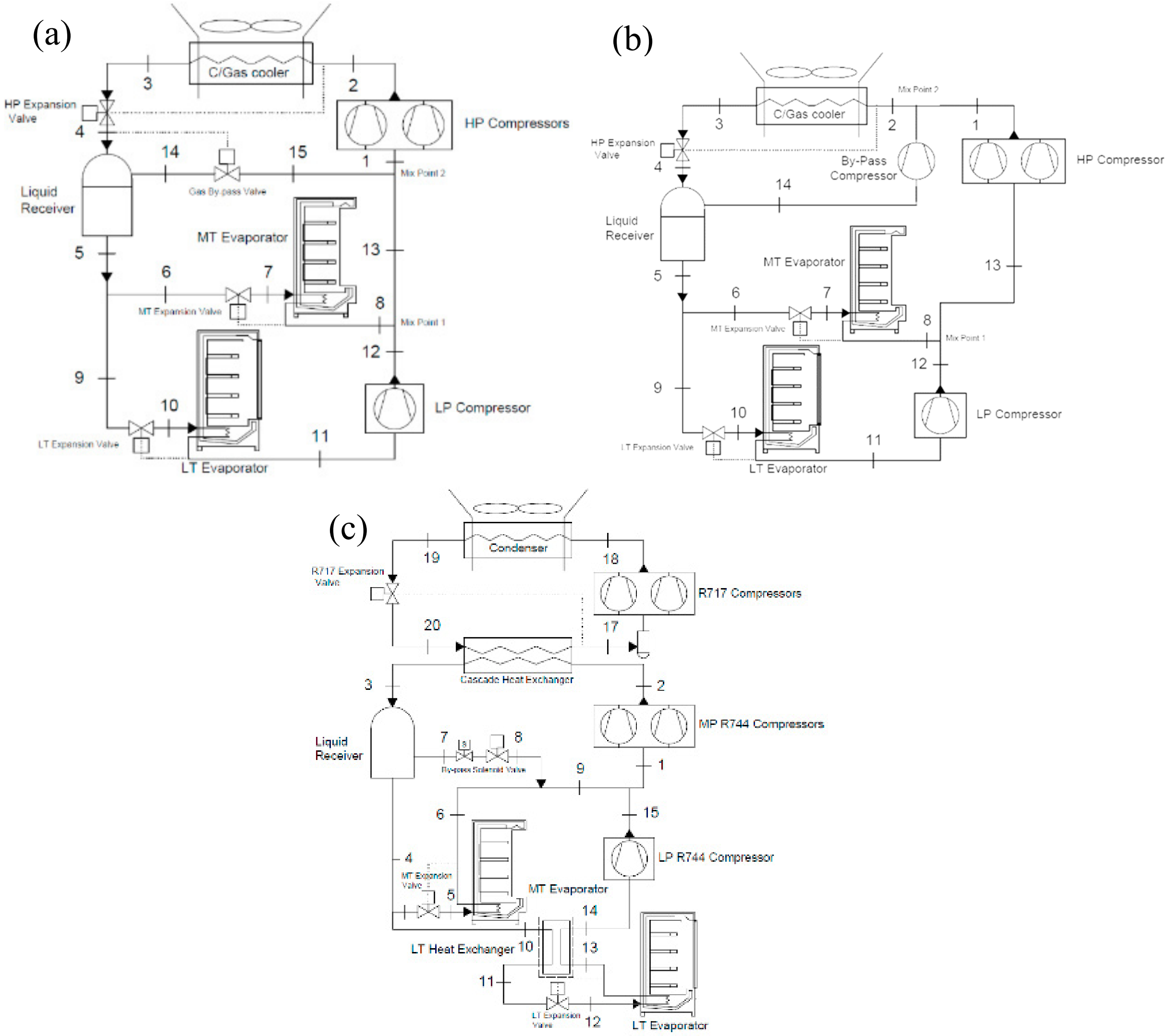

Fig. 1. Schematic diagram of (a) Booster System, (b) Parallel-Compressor Booster System, and (c) Cascade System.

3. Thermodynamic model details

To assess the performance of the selected systems, the parameters used in the simulation of the three configurations are presented in Table 1. The power consumption of the MT/LT evaporators fans, lights, and other electrical devices including the defrost system were set to 14 kW, while the condenser/gas cooler fan power consumption was set to 5 kW [14]. For the case when cooling loads were set to 25 kW (MT) and 5 kW (LT), the power consumption of the mentioned devices were set to 4 kW and 1.5 kW, respectively. The Engineering Equation Solver software was used for the modelling [21].

Table 1. Input thermodynamic conditions.

Cascade R717/R744 Parameters	Values	(Typical and Parallel) Booster R744 Parameters	Values
Condenser approach temperature difference, K	5	Condenser/Gas Cooler outlet temperature conditions	[14]
Cascade HX Temperature Difference, K	5	Condenser/Gas Cooler outlet pressure conditions	[14]
LT Heat Exchanger Effectiveness	0.4	Intermediate pressure, Bar	35
MT Evaporator Cooling Load, kW	120, 25	MT Evaporator Cooling Load, kW	120, 25
LT Evaporator Cooling Load, kW	25, 5	LT Evaporator Cooling Load, kW	25, 5
MT Evaporating Temperature, °C	-10	MT Evaporating Temperature, °C	-10
LT Evaporating Temperature, °C	-32	LT Evaporating Temperature, °C	-32
Air Temperature at the Inlet of the MT Evaporator, °C	5	Air Temperature at the Inlet of the MT Evaporator, °C	5
Air Temperature at the Inlet of the LT Evaporator, °C	-18	Air Temperature at the Inlet of the LT Evaporator, °C	-18
Superheating at the MT and LT Evaporators, K	7	Superheating at the MT and LT Evaporators, K	7

Each refrigeration system was simulated performing mass and energy balances on each of the components of the system. The thermodynamic analysis of each system was conducted assuming that the refrigeration system operates under steady-state conditions and that pressure drops, kinetic and potential energy through the system components are negligible, and so are heat and friction losses. Applying the first law of thermodynamics, the coefficient of performance of the refrigeration systems is expressed as:

$$COP = \frac{\dot{Q}_{MT}+\dot{Q}_{LT}}{\dot{W}_{Total}} \quad (1)$$

$$\dot{W}_{Total} = \dot{W}_{compressors} + \dot{W}_{fans,lights,others} \quad (2)$$

Where $\dot{Q}_{MT}$ and $\dot{Q}_{LT}$ are the medium and low temperature evaporators cooling loads, respectively. $\dot{W}_{Total}$ is the total power input due to the compressors, fans, lights and other electrical devices in each system. The isentropic efficiency of the R717 compressor was estimated employing the correlations (3) as in [13]. In the case of the R744 compressors, correlation (4) was used for medium and low pressure compressors, respectively [13].

$$\eta_{comp,R717} = -0.00097{P_R}^2 - 0.01026P_R + 0.83955 \quad (3)$$

$$\eta_{comp,R744} = 0.00476{P_R}^2 - 0.09238P_R + 0.89810 \quad (4)$$

Where $P_{R,}$ is the pressure ratio of the compressor.

Table 2 shows the mass and energy balances for each component in the cascade system. Exergy analysis, was performed on each system in order to quantify reversibility rates and identify the critical components of the system that need to be improved. The energetic efficiency of the selected refrigeration systems applying the second law of the thermodynamics can be expressed as follows:

$$\eta_{ex} = 1 - \frac{\dot{I}_D}{\dot{E}_{in}} \quad (5)$$

where $\dot{E}_{in}$ is the total inlet exergy, $\dot{I}_D$ stands for the total exergy destruction or irreversibility. For each system, $\dot{E}_{in}$ can be approximated as the total work input while $\dot{I}_D$ can be estimated as the summation of the irreversibility in each one of the components.

The irreversibility in each one of the components was calculated as summarised in Table 2.

Table 2. Energy balances and irreversibility in each component of the selected refrigeration systems.

Components	Mass Balances	Energy Balances	Exergy Balances
Condensers	$\dot{m}_{in} = \dot{m}_{out}$	$\dot{Q}_{Cond} = \dot{m}_{in}h_{in} - \dot{m}_{out}h_{out}$	$\dot{I}_{Cond} = \dot{m}_{in}(h_{in} - h_{out} - T_{amb,K}(s_{in} - s_{out}))$
Expansion Valves	$\dot{m}_{in} = \dot{m}_{in}$	$\dot{m}_{in}h_{in} = \dot{m}_{out}h_{out}$	$\dot{I}ev = \dot{m}_{in}T_{amb,K}(s_{out} - s_{in})$
Compressors	$\dot{m}_{in} = \dot{m}_{out}$	$\dot{W}_{Comp} = (\dot{m}_{out}h_{out,S} - \dot{m}_{in}h_{in})/\eta_{comp,R717}$	$\dot{I}comp = \dot{m}_{in}T_{amb,K}(s_{out} - s_{in})$
Heat exchangers	$\dot{m}_{A,in} = \dot{m}_{A,out}$ $\dot{m}_{C,out} = \dot{m}_{C,out}$	$\dot{m}_{C,in}h_{C,in} + \dot{m}_{A,in}h_{A,in} = \dot{m}_{C,out}h_{C,out} + \dot{m}_{A,out}h_{A,out}$	$\dot{I}_{HE} = T_{amb,K}(\dot{m}_{A,out}(s_{A,out} - s_{A,in}) + (\dot{m}_{C,in}(s_{C,out} - s_{C,in}))$
Evaporators	$\dot{m}_{in} = \dot{m}_{out}$	$\dot{Q}_{Ev} = \dot{m}_{out}h_{out} - \dot{m}_{in}h_{in}$	$\dot{I}e = \dot{m}_{in}T_{amb,K}(s_{out} - s_{in} + (h_{in} - h_{out})/T_{a,MT/LT,K}))$

4. Results and discussion

The energy analysis results in Fig. 2a, show that the cascade system COP was found to be higher than the typical booster and parallel-compressor booster system when the ambient temperature is above 4 °C and 16 °C, respectively. Moreover, the fact that the R744 flows on the low-side of the cascade system and is condensed by the cascade heat exchanger, it ensures the subcritical operation over the whole year without being affected by the ambient temperature. In this case, the receiver is fed with liquid R744 all the time without the need of by-pass. It is also noted that the decrease of the COP is more pronounced for both the booster systems in comparison to the cascade system and that their performance are similar from the ambient temperature of 26 °C. As shown in Fig. 2a, the more drastic reduction of the COP in both the booster systems is due to a sharper increase in the power consumption of the systems.

The increase in the power consumption of the booster systems can be explained due to the fact that the amount of the refrigerant by-pass from the receiver to suction line is significantly increased as the ambient temperature increases. This overloads the MP compressors leading to higher power consumption of these components, and therefore, the power consumption of the whole booster system. Regarding the cascade system, it is shown that the power consumption varies slightly since the R744 low-side of the cascade system is not affected by the ambient temperatures. In the case of the R744 side, just a very small variation in the compressor power consumption is noted as the ambient temperature increases leading to the same effect on the total power consumption of the system. On the other hand, Fig. 2b shows that for convenience store application with 30 kW total cooling capacity the switch point between the performance of the parallel-compressor booster and cascade systems moves to an ambient temperature of 26 °C which limit the application temperature range of the cascade configuration for low thermal capacity systems.

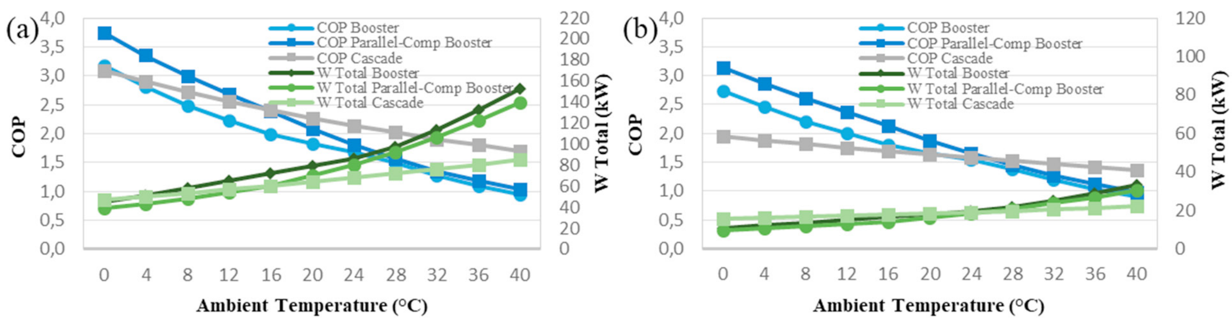

Fig. 2. Ambient temperature vs. COP and total energy consumption for the selected systems for (a) MT load of 120 kW and LT of 25 kW, and for (b) MT load of 25 kW and LT of 5 kW.

The exergy analysis, Fig. 3, shows the second law efficiency and the exergy destruction percentage per component in each system with a total cooling load of 145 kW at an ambient temperature ranging from 0 to 40 ºC. Fig. 3a shows the typical booster system modelling results which indicate that the second law efficiency decreases from 0.413 to 0.263 for the given temperature range where the main drop in efficiency is noted from a temperature of 26 °C. A similar behaviour is observed in the efficiency of the parallel-compressor booster system which decreases from 0.485 to 0.293. In this system the exergy efficiency decreases almost linearly from 16 °C. In the case of the cascade configuration, Fig. 3c, shows that the second law efficiency increases from 0.411 to 0.475. It is noted that for the booster systems, the total exergy destruction rate increment is more significant than that of the power input increase with the ambient temperature increase. In addition, for the typical booster system a more pronounced increment in exergy destruction is observed from the temperature above 26 °C. In the case of the cascade system, it shows an opposite effect, which means that the total exergy destruction rate increment was slightly lower than that of the required energy input when the ambient temperature increases.

It is also observed that the condenser is the most critical component of the cascade configuration followed by the MT evaporator. Fig. 3c shows that the exergy destruction rate in the condenser of the cascade system varies from 6.25 to 10.94 $kJ.s^{-1}$ while it just varies from 6.6 to 7.6 in the MT evaporator. On the other hand, the MT compressor, the gas cooler, the expansion valve located after the gas cooler, and the by-pass compressor in the case of the advanced booster system, appear to be the components with the highest exergy destruction when the ambient temperature rises above 26 °C. Fig. 3a shows that the exergy destruction rate in the MT compressor of the typical booster system varies from 4.8 to 18.0 $kJ.s^{-1}$ for an ambient temperature ranging from 0 to 26 °C, then it presents a sharper increase up to 41.6 $kJ.s^{-1}$ for a temperature of 40 °C. A similar behaviour is observed in the gas cooler and expansion valve after the gas cooler showing exergy destruction rates from 9.3 to 26.4 $kJ.s^{-1}$ and from 1.0 to 23.1 $kJ.s^{-1}$, respectively.

With regards to the parallel-compressor booster system, Fig. 3b shows that the exergy destruction rates in each component are lower if compared with those of the typical booster one. In this case, the maximum exergy rate is obtained in the gas cooler ranging from 5.6 to 26.4 $kJ.s^{-1}$ for the given ambient temperature interval. The exergy destruction in the MT compressor and expansion valve after the gas cooler vary from 3.2 to 22.71 $kJ.s^{-1}$ and from 0.52 to 24.3 $kJ.s^{-1}$, respectively. In the case of the other components, it is noted that the exergy destruction keeps almost constant which means that those components are not significantly affected by the ambient temperature increase.

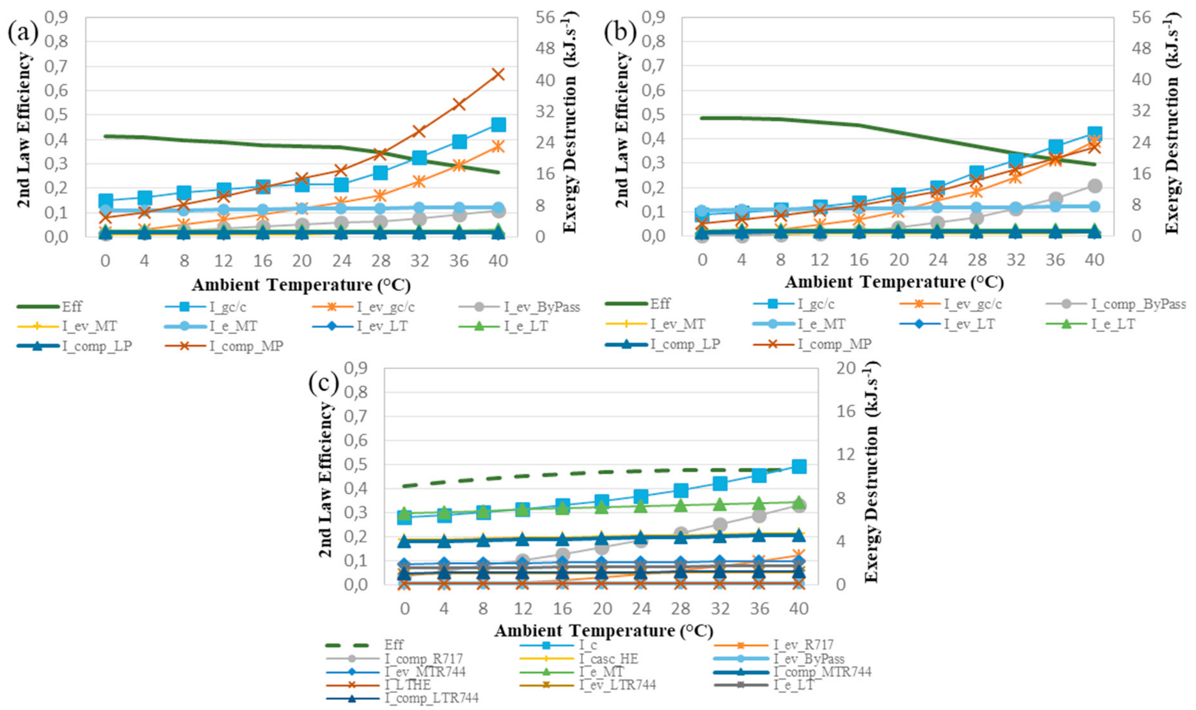

Fig. 3. Ambient Temperature vs. 2nd Law Efficiency and Exergy Destruction Rate for (a) Booster System, (b) Parallel-Compressor Booster System, and (c) Cascade System.

5. Conclusions

The main conclusions from the present study are: The conventional R744 booster configuration and R744 parallel-compressor booster systems demonstrated better performance than the cascade system at ambient temperatures up to 2 °C and 14 °C, respectively. Above these temperatures, the cascade system performance was found to be better than the two booster systems.

It was also found that for a convenience store application with a 30 kW total cooling capacity, the switch point for better performance by a cascade system rises to an ambient temperature of 26 °C which limits the applications of the cascade system to low capacity applications.

With regards to the second law analysis, the efficiency of both booster systems decreased with the ambient temperature due to high exergy destruction rates especially at temperatures above 26 °C. The opposite effect was observed for the cascade system. The amount of exergy destruction in the MT compressor, gas cooler and expansion valve after the gas cooler accounted for a large percentage in the total exergy destruction for both the booster systems, making them the most critical components. In the case of the cascade system, the condenser and the MT evaporator were identified as the most critical components.

Acknowledgements

The authors acknowledge the funding from the Research Councils UK for the research, Grant No: EP/K011820/1. Data used in the analysis can be found in the paper but if more data or information is required, they can be obtained from the corresponding author.

References

[1] Parpas D., Amaris C., Sun J., Tsamos K., Tassou S., "Numerical study of air temperature distribution and refrigeration systems coupling for chilled food processing facilities." Energy Procedia, 123 (2017): 156-163
[2] Parpas D., Amaris C., Tassou S.A., "Investigation into air distribution systems and thermal environment control in chilled food processing facilities." International Journal of Refrigeration 87 (2018): 47-64.
[3] Lee T.S., Liu C.H., Chen T.W. "Thermodynamic analysis of optimal condensing temperature of cascade-condenser in CO2/NH3 cascade refrigeration systems." International Journal of Refrigeration 29 (2006): 1100-1108
[4] Bingming W., Huagen W., Jianfeng L., Ziwen X. "Experimental investigation on the performance of NH3/CO2 cascade refrigeration system with twin-screw compressor." International Journal of Refrigeration 32 (2009): 1358-1365.
[5] Dopazo J.A., Fernández-Seara J., Sieres J., Uhía F.J. "Theoretical analysis of a CO2– NH3 cascade refrigeration system for cooling applications at low temperatures." Applied Thermal Engineering 29 (2009): 1577-1583.
[6] Rezayan A., Behbahaninia A. "Thermoeconomic optimization and exergy analysis of CO2/NH3 cascade refrigeration systems." Energy 36 (2011): 885-895.
[7] Messineo A. "R744-R717 Cascade Refrigeration System: Performance Evaluation compared with a HFC Two-Stage System." Energy Procedia 14 (2012): 56-65.
[8] Sawalha S. "Theoretical evaluation of trans-critical CO2 systems in supermarket refrigeration. Part I: Modelling, simulation and optimization of two system solutions." International Journal of Refrigeration 31 (2008): 516-524.
[9] Mosaffa A.H., Garousi Farshi L., Infante Ferreira C.A., Rosen M.A. "Exergoeconomic and environmental analyses of CO2/NH3 cascade refrigeration systems equipped with different types of flash tank intercoolers." Energy Conversion and Management 117 (2016): 442-453.
[10] Sun Z., Liang Y., Liu S., Ji W., Zang R., Liang R., Guo Z. "Comparative analysis of thermodynamic performance of a cascade refrigeration system for refrigerant couples R41/R404A and R23/R404A." Applied Energy 184 (2016): 19–25.
[11] Nasruddin N., Sholahudin S., Giannetti N., Arnas. "Optimization of a cascade refrigeration system using refrigerant C3H8 in high temperature circuits (HTC) and a mixture of C2H6/CO2 in low temperature circuits (LTC)." Applied Thermal Engineering 104 (2016): 96-103.
[12] Kilicarslan A., Hosoz M. "Energy and irreversibility analysis of a cascade refrigeration system for various refrigerant couples." Energy Conversion and Management 51 (2010): 2947–2954.
[13] Lee T.S., Liu C.H., Chen T.W. "Thermodynamic analysis of optimal condensing temperature of cascade refrigeration systems." International Journal of Refrigeration 29 (2006): 1100 - 1108.
[14] Tsamos K.M., Ge Y.T., Santosa ID.M.C., Tassou S.A., Bianchi G., Mylona Z. "Energy analysis of alternative refrigeration system configurations for retail food applications in moderate and warm climates." Energy Conversion and Management 150 (2017): 822-829.
[15] Ge Y.T., Tassou S.A. "Thermodynamic analysis of transcritical CO2 booster refrigeration systems in supermarket." Energy Conversion and Management 52 (2011): 1868-1875.
[16] Gullo P., Elmegaard B., Cortella G. "Advanced exergy analysis of a R744 booster refrigeration system with parallel compression." Energy 107 (2016): 562-571.

[17] Gullo P., Elmegaard B., Cortella G. "Energy and environmental performance assessment of R744 booster supermarket refrigeration systems operating in warm climates." International Journal of Refrigeration 64 (2016): 61-79.
[18] Gullo P., Hafner A., Cortella G. "Multi-ejector R744 booster refrigerating plant and air conditioning system integration – A theoretical evaluation of energy benefits for supermarket applications." International Journal of Refrigeration 75 (2017): 164-176
[19] Mylona Z., Kolokotroni M., Tsamos T. M., Tassou S.A., "Comparative analysis on the energy use and environmental impact of different refrigeration systems for frozen food supermarket applications." Energy Proceedia 123 (2017): 121-130.
[20] Amaris C., Tsamos K. M., Ge Y., Tassou S. A. "Thermodynamic analysis on the performance of an R717/R744 cascade refrigeration system for food retail applications." 16th International Conference on Sustainable Energy Technologies – SET 2017 (2017).
[21] EES, Engineering Equation Solver, version 9.810, 2014. www.fChart.com